An outdoor navigation system using GPS and inertial platform

S. Panzieri† F. Pascucci‡ G. Ulivi†

†Dipartimento di Informatica e Automazione
Università degli Studi "Roma Tre"
Via della Vasca Navale 79, 00146 Roma, Italy
{panzieri,ulivi}@uniroma3.it

‡Dipartimento di Informatica e Sistemistica
Università degli Studi "La Sapienza"
Via Eudossiana 18, 00184 Roma, Italy
pascucci@dia.uniroma3.it

Abstract— **The use of Global Positioning System (GPS) in outdoor localization is a quite common solution in large environments where no other references are available and positioning requirements are not so pressing. Of course, fine motion without the use of an expensive differential device is not an easy task even now that available precision has been greatly improved as the military encoding has been removed. In this paper we present a localization algorithm based on Kalman filtering that tries to fuse information coming from an inexpensive single GPS with inertial and, sometimes uncertain, map based data. The algorithm is able to produce an estimated configuration for the robot that can be successfully fed back in a navigation system, leading to a motion whose precision is only related to current information quality. Some experiments show difficulties and possible solutions to this sensor fusion problem.**

I. Introduction

Outdoor navigation is an exciting and quite varied topic; there are several types of environment that require different levels of autonomy and different kind of sensors. A vehicle traveling in a wood shows requirements that are not needed by one exploring a parking lot; both, however, are doing outdoor navigation. In this paper we shall address the latter situation that seems to be more promising for applications; surveillance, cleaning, moving goods, and even searching for a specific item (a car, a container) are operations that can be, in a near future, assigned to outdoor robots. By the way, such units could be freed from the usual energy shortage, because they can adopt fuel instead of batteries as the primary power supply.

Even in this rather simple environment, problems are very different from those encountered in indoor navigation; indeed, the required sensors must be different; as an example, ultrasonic sensors cannot be used, being them affected by rain and wind and having them, anyway, a too short range. However, the greatest difference is the kind of *a priori* knowledge that can be used for localization, a skill required also outdoors. Indeed, the typical environment features used indoors for this purpose are quite scarce outdoors, moreover, large, stationary obstacles can appear and disappear: consider, e.g., the effect of some cars parked in front of a wall. When perceived by the exteroceptive sensors, they can either be interpreted as the wall itself (and therefore produce an erroneous localization) or cause the distance measures to be discarded (so reducing the amount of available information).

Outdoors, the Global Position System (GPS) is an interesting possibility to cope with these problems without adding special devices as reflectors or targets. Till May 1st of this year, the available precision was downgraded for military reasons, so that only differential receivers could be used for localization; now the full satellite precision can be achieved with a simple, cheap unit. It requires very little data processing and its error is independent from the traveled distance and from the positions of the obstacles. The problem is, therefore, to characterize the performance of this system in different situations and to adapt the localization and the navigation systems to get the maximum benefit from its use.

The paper is devoted to analyze the localization system implemented for an ATRV-Jr unit that has to move in a parking lot on a paved but rather rugged terrain. After a brief description of the available exteroceptive sensors, the accuracy of the GPS is discussed in some detail on the basis of some experiments. Indeed, this is the most important sensor for large movements in open spaces, when no other reference is available and its short-term error affects the implementation of the entire navigation system. The localization system is based on an Extended Kalman Filter, it is described giving emphasis to the peculiarities arising from characteristics of the used sensors. Finally, some guidelines are given to design the planner according to the EKF achievable performance and the nature of the environment. The description of an experimental result concludes the paper.

II. Performance of a simple GPS system

A GPS receiver relies on the signal received from several satellites that are not geostationary. Therefore, the number and the position of the available satellites change in time influencing the system precision. Several information are available on sources of GPS errors; often they refer to long-term averages and/or to high quality receivers that cannot be employed on a mobile robot.

To understand the level of precision and the error behaviour when using an inexpensive receiver (we used the Garmin GPS35-HVS), some experiments have been conducted in the parking lot of our department. We chose two places, say points A and B; the first was far from obstacles affecting the wave propagation, the other was in a sort of corridor, delimited by two buildings. The robot was placed

still in the two points where it acquired data in different hours of the day. All the acquisitions lasted 15 minutes, during which measures were collected with a sampling period of 1 second, resulting in 900 measures per acquisition. The first two tables refer the satellite availability in the two points. As it can be seen, the number of available satellites is quite different in the two points, being the most probable value 7 in the open location and 5 in the partially covered one. Note that 4 satellites is the minimum number for a complete 3D localization.

TABLE I
SATELLITE AVAILABILITY AT POINT A

Satellite number	First acquisition	Second acquisition	Overall percentage
4	0	11	0.6
5	0	53	2.9
6	197	127	18.0
7	685	282	53.7
8	18	427	24.7

TABLE II
SATELLITE AVAILABILITY AT POINT B

Satellite number	First acquisition	Second acquisition	Third acquisition	Overall percentage
3	180	0	0	6.6
4	401	298	121	30.3
5	319	602	697	59.9
6	0	0	82	3.0

The next two tables relate the Standard Deviation of the measures for each acquisition, computed according to the number of satellites and for all the measures.

Observing these tables, it easy to understand that the number of satellites provides just a very rough indication of the accuracy of the measure (look, in particular, at row 5 of Tab. II). Indeed, a different indicator should be available, the Dilution of Precision (DOP), which is based on the satellite geometry in sky, but the installed driver we have does not return this information. This is shown by the Fig. 1 and Fig. 2 , where the two acquisition in point A are plotted with different symbols according to the number of satellites.

TABLE III
STANDARD DEVIATION (M) AT POINT A

Satellite number	First acquisition		Second acquisition	
	E-W	S-N	E-W	S-N
4	-	-	1.0	3.5
5	-	-	1.2	3.6
6	2.3	1.1	1.9	4.2
7	2.1	1.7	2.6	4.1
8	0.4	0.0	1.0	2.3
Total	2.2	1.7	2.3	4.2

TABLE IV
STANDARD DEVIATION (M) AT POINT B

Satellite number	First acquisition		Second acquisition		Third acquisition	
	E-W	S-N	E-W	S-N	E-W	S-N
3	3.8	11.4	-	-	-	-
4	2.9	7.2	2.4	1.1	2.9	3.3
5	2.0	3.2	1.9	0.7	10.0	7.6
6	-	-	-	-	0.8	0.7
Total	3.0	7.9	2.4	0.9	10.8	9.2

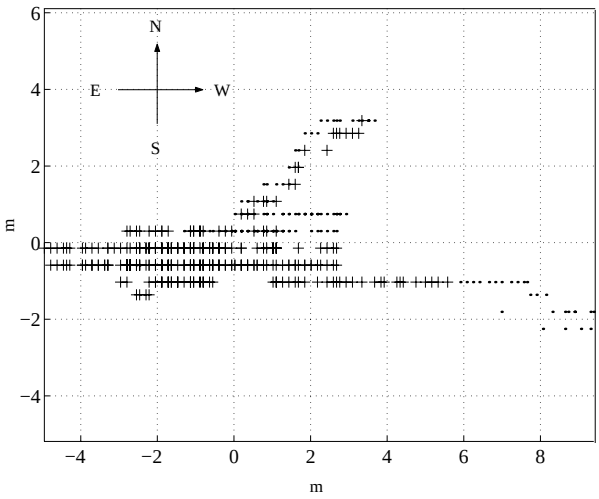

Fig. 1. First acquisition at point A. Number of satellite: dot 4, plus 5, circle 6

As it can be seen, there is a lack of resolution in one direction, because the available satellites are aligned. Only the addition of the 6-th satellite, which probably was not aligned, allows a remarkable increase of precision, as it can be shown by the positions of the circles.

Another important point is the way the error changes in time, i.e., if it is white or colored. A fast changing error can be better filtered, but its residue adds some random motion to the one desired for the robot. On the contrary, a slow varying one cannot be removed in short time, but allows for a smoother movement; moreover it should be considered that we are interested in the relative position accuracy, as here and there the robot finds some environment feature to improve its localization.

An easy way to look at the phenomenon is to plot the "path" of the measured position for a given number of satellites. Looking at Fig. 3 (obtained for 5 satellites), it is easily understood that successive errors are tightly related, and therefore the error is strongly colored, in particular when the errors are large. A better characterization is shown by the auto-correlation function that is not reported here for sake of space. Moreover, in this case, there is also a strong correlation between E-W errors and N-S errors. ¿From these considerations we can conclude that changing the co-

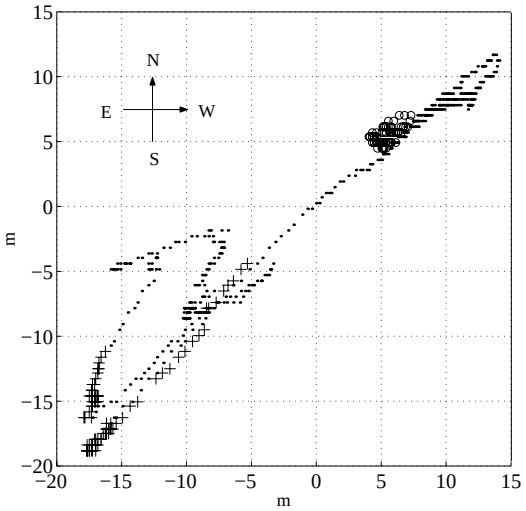

Fig. 2. Second acquisition at point A. Number of satellite: plus 4, dot 5, circle 6

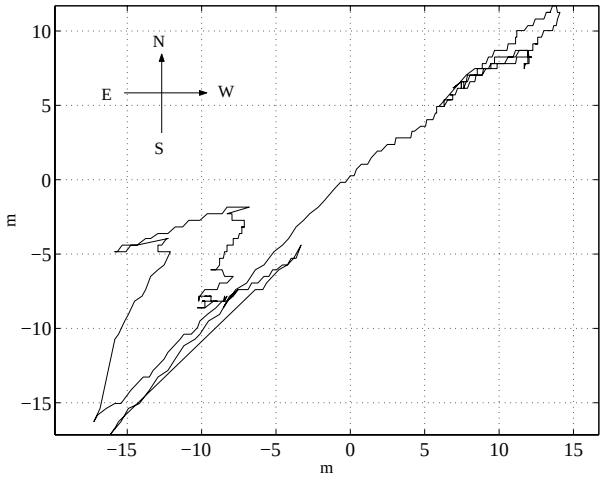

Fig. 3. Second acquisition at point A. Error path for 5 satellites

variance matrix of the GPS according to the number of satellites is of little or no help in improving the overall precision, whilst this could be done if the satellite geometry were available.

Moreover, as the error is slow varying, approaching once in a while some known environment feature can reset the overall error and keep it bounded at a value lower than the expected one.

III. The localization system

We consider a mobile robot with differential drive kinematics [6], described by the following equation:

$$\begin{pmatrix} \dot{x} \\ \dot{y} \\ \dot{\theta} \end{pmatrix} = \begin{pmatrix} cos\theta \\ sin\theta \\ 0 \end{pmatrix} v + \begin{pmatrix} 0 \\ 0 \\ 1 \end{pmatrix} \omega. \qquad (1)$$

The motion is generated by four tires, actuated by two independent motors. The robot location (i.e. robot configuration [3]) is given by $x = (p^x, p^y, \phi)$, where p^x, p^y are the cartesian coordinates of the vehicle center and ϕ is the mobile platform orientation with respect to the x-axis.

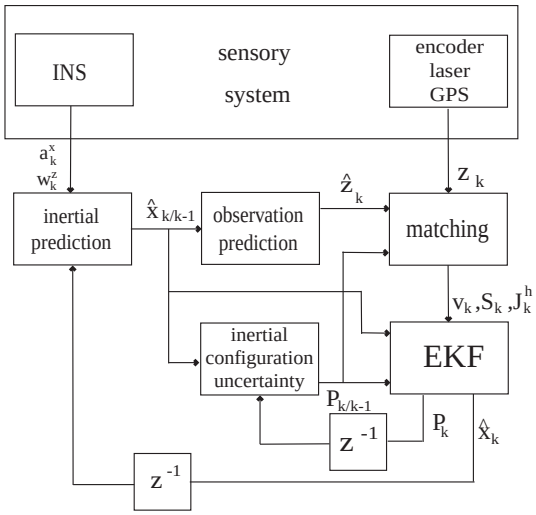

Fig. 4. Structure of the localization system (z^{-1} denotes the unit delay operator)

The on-board sensory system includes two incremental encoders measuring the rotation of each motor, a inertial navigation system that provides measures of the robot linear accelerations and angular velocities, a laser scanner which measures the distances between a fixed point on the robot body and obstacle surfaces in the environment, and a GPS antenna measuring absolute position in the geodetic coordinates.

The structure of our localization system, shown in Fig. 4, proceeds directly from the EKF equations [2]. At the k-th step, the kinematic model of the robot is used to compute an inertial prediction $\hat{x}_{k/k-1}$ and an associated covariance matrix $P_{k/k-1}$; an observation prediction $\hat{z}_k$ is formed and compared with the measure z_k provided by the sensory system. The results are the innovation term v_k and its covariance matrix S_k, that are used by the EKF to produce the state estimate $\hat{x}_k$ and the new associated covariance P_k.

A. Inertial prediction

Define the state vector as $x = (p^x, p^y, \phi, v, b)$ where v is the linear velocity of the vehicle and b denotes the accelerometer bias [5]. The rate gyro bias is constant, so we estimate it only at the beginning of the navigation (see [8] for an algorithm estimating gyro bias). The inputs of the inertial model are $u_k = (a_k^x, \omega_k^z)^T$ where a_k^x is the mean robot acceleration along the motion direction and ω_k^z is the mean angular velocity during the k-th sampling interval. The inertial prediction is then

$$\hat{x}_{k/k-1} = \begin{bmatrix} 1 & 0 & 0 & \Delta t_k \cos\tilde{\phi}_k & -(\frac{\Delta t_k{}^2}{2})\cos\tilde{\phi}_k \\ 0 & 1 & 0 & \Delta t_k \sin\tilde{\phi}_k & -(\frac{\Delta t_k{}^2}{2})\sin\tilde{\phi}_k \\ 0 & 0 & 1 & 0 & 0 \\ 0 & 0 & 0 & 1 & -\Delta t_k \cos\tilde{\phi}_k \\ 0 & 0 & 0 & 0 & 1 \end{bmatrix} \hat{x}_{k-1} +$$

$$+\begin{bmatrix} (\frac{\Delta t_k}{2}^2)\cos\tilde{\phi}_k & 0 \\ (\frac{\Delta t_k}{2}^2)\sin\tilde{\phi}_k & 0 \\ 0 & \Delta t_k \\ \Delta t_k & 0 \\ 0 & 0 \end{bmatrix} u_k = f(\hat{x}_{k-1}, u_k, \Delta t_k) \quad (2)$$

where $\tilde{\phi}_k = \phi_{k-1} + (1/2)\omega_k^z \Delta t_k$ is the average vehicle orientation during the sampling interval Δt_k. The covariance matrix associated with the prediction error is written as

$$P_{k/k-1} = J_x^f(\hat{x}_{k-1})\, P_{k-1}\, (J_x^f(\hat{x}_{k-1}))^T + J_u^f(u_k)\, C\, (J_u^f(u_k))^T + Q. \quad (3)$$

Here, $J_x^f(\cdot)$ and $J_u^f(\cdot)$ are the Jacobian matrices of $f(\cdot)$ with respect to $\hat{x}_{k-1}$ and u_k, P_{k-1} is the covariance matrix at time instant t_{k-1}, $C = \text{diag}\{\sigma_{ax}^2, \sigma_{\omega z}^2\}$ is the covariance matrix of the gaussian white noise which corrupts the input measure and $Q = \text{diag}\{\sigma_{px}^2, \sigma_{py}^2, \sigma_{p\phi}^2, \sigma_v^2, \sigma_b^2\}$ is the covariance matrix of the gaussian white-noise which directly affects the state in the kinematic model.

B. Observation prediction and matching

The observation prediction consists of subvectors $\hat{z}_k^e$ (predicted encoder velocity), $\hat{z}_k^l$ (predicted laser readings), $\hat{z}_k^{gps}$ (predicted robot position by GPS). For the observation prediction $\hat{z}_k^e$, we simply let

$$\hat{z}_k^e = h^e(x_{k/k-1}) = \hat{v}_{k/k-1}. \quad (4)$$

The observation prediction of the laser measure is computed over a given environment map $\mathcal{M}$ and the inertial prediction $\hat{x}_{k/k-1}$

$$\hat{z}_k^l = h^l(\hat{x}_{k/k-1}, \mathcal{M}). \quad (5)$$

We shall not detail here the above computation. It should be noted that h reflects the way in which the environment map is represented - in our case, a list of segment [4] - as well as the model interaction between the environment itself and the laser scanner. The subvector $\hat{z}_k^{gps}$ is written as

$$\hat{z}_k^{gps} = h^{gps}(x_{k/k-1}) = \begin{pmatrix} \hat{p}_{k/k-1}^x \\ \hat{p}_{k/k-1}^y \end{pmatrix}. \quad (6)$$

In (6), we consider a conversion of the GPS measure from geodetic coordinates to the environment framework.

The innovation term and the associated covariance, being $\hat{z}_k = (\hat{z}_k^e, \hat{z}_k^l, \hat{z}_k^{gps})$ and z_k the measured outputs, are then computed as

$$v_k = z_k - \hat{z}_k \quad (7)$$

$$S_k = J_x^h(\hat{x}_{k/k-1})\, P_{k/k-1}\, (J_x^h(\hat{x}_{k/k-1}))^T + R_k \quad (8)$$

where $J_k^h(\cdot)$ is the Jacobian matrix of $h = (h^e, h^l, h^{gps})$ respect to $x_{k/k-1}$. The first term used to compute S_k represents the uncertainty on the observation due to the uncertainty on the inertial prediction. The second term is the observation noise covariance matrix.

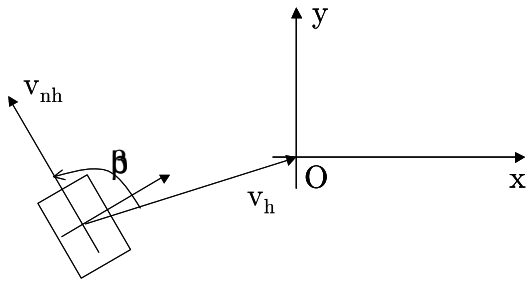

Fig. 5. Holonomic and nonholonomic velocities

The measurement noise depends on the interaction between the sensor system and the environment, which is not invariant in space and time. For example some surfaces (glass or hedges) are more difficult to detect for laser sensor. To model this fact, we have chosen to label each segment of the map with a value representing the reliability of the laser measure provided by that segment, and to modify the corrispondent rows of the covariance matrix R accordingly [7]. Also the GPS rows of R are modified by the number of satellite that the antenna uses at the istant time t_k, because the sensor accuracy depend on their number and position.

Moreover to avoid the inclusion of outliers in the correction phase, we need to set up for the laser measure a *validation gate* as follows [1]. Suppose that $v_{k,j}$ is the innovation term for a laser ray; it will be passed to the EKF only if

$$\frac{v_{k,j}^2}{s_j} \leq \gamma^2 \quad (9)$$

where s_j is the j-th diagonal term of S and parameter γ should be tuned by experimental trials. In the same way GPS measure obtained using less than four satellite are discharged.

C. Extended Kalman Filter

The Extended Kalman Filter is used to correct the inertial configuration estimate one the basis of the validated observations. Particularly, the final configuration estimate is obtained as

$$\hat{x}_k = \hat{x}_{k/k-1} + K_k[z_k - \hat{z}_k] \quad (10)$$

where K_k is the Kalman gain matrix

$$K_k = P_{k/k-1}(J_x^h(\hat{x}_{k/k-1}))^T S_k^{-1}. \quad (11)$$

The covariance associated with the final configuration estimate $\hat{x}_k$ is given by

$$P_k = P_{k/k-1} - K_k\, S_k\, K_k^T. \quad (12)$$

IV. Planning and control

As explained before, the GPS provides the position of the robot with a maximum error that can be as high as 20 meters, even if generally this is quite lower. If the trajectory proceeds for a long time far from any reference point,

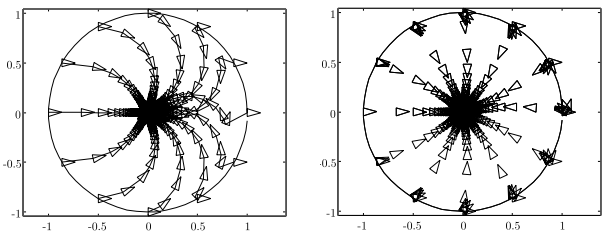

Fig. 6. Trajectories without (left) and with (right) forward cut off

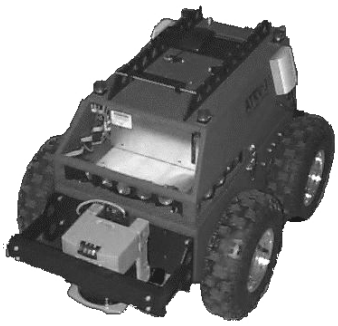

Fig. 7. The mobile robot ATRV-Jr

the position error can reach that value. If the range of the other exteroceptive sensors is larger than the actual position error, then this can be corrected when a feature appears in the robot field of view. Otherwise, as it happens in our case, there is the possibility that the error cannot be corrected. This event is uncommon, and its occurrence can be avoided by planning a path that passes near some environment feature before the errors grow too large, even if in this way the minimum length property is missed. Moreover, if the DOP is available, this behaviour can be activated only when needed, perhaps by a real time trajectory reconfiguration.

Thereafter, the proposed solution has been the one of specifying the path as a sequence of via-points to be attained using, for example, a simple static time-invariant feedback control law on each segment. It is well known that, for nonholonomic systems like unicycle robots, the point tracking problem, i.e., tracking of only cartesian coordinates, can be solved using a partial feedback linearization of the dynamic model and a simple PD like control law in the new coordinates [10]. If we suppose that both exact tracking along each segment and a particular posture at the via-point are not required, the problem can be relaxed to the stabilization of only the first two coordinates of system (1). This could be attained with an easy strategy, obtained by simplifying the one presented in [11]: first of all (see Fig. 5) define a suitable holonomic velocity v_h, unaware of the nonholonomic constraint, able to perform the stabilizing task, i.e., able to steer the origin of the robot frame over the origin O of the reference frame; second, define two control laws one as projection of v_h along the nonholonomic direction v_{nh} and the other steering the nonholonomic axis of the vehicle towards the holonomic velocity vector (to reduce β)

$$v = K_e \parallel v_h \parallel cos(\beta) \quad (13a)$$

$$\omega = -K_\omega \beta. \quad (13b)$$

The convergence to the origin can be easily proved considering that eq. 13b independently steers the angle ϕ to a value that will definitively let $\beta = 0$. Now, using a Lyapunov candidate $V(x, y) = x^2 + y^2$ it is easy to see that its derivative is, when $\beta = 0$, $\dot{V} = -2K_e(x^2 + y^2)$, and is negative defined. At the left of Fig. 6 trajectories generated for different starting points are reported. To avoid back motion a different strategy has been applied and its results reported at the right of the same figure: the first control has been set at zero until $\parallel \beta \parallel$ is less than a threshold of $10deg$. In this case trajectories are more linear and, for this reason, this strategy has been implemented. The only point where this control fails is the origin itself where β is undefined but to avoid also strong discontinuities in the control law, possibly caused by sudden corrections of the estimated position due to new available laser measures, the via-points have been defined as a circular region of radius 0.5m and the robot has been forced to halt when it steps into this region.

Finally, to take into account the presence of obstacles, has been added an obstacle avoidance module whose description can be found in [9].

V. Experimental results

The proposed algorithm has been tested on the mobile robot ATRV-Jr produced by Real World Interface (see Fig. 7). The robot has four tires, actuated by two independent motors, so the kinematic model of the platform is a differential drive one. The sensory system is composed by two incremental encoders mounted on the two motors, a 180 degrees view laser scanner (LMS-Sick), a GPS (Garmin GPS35-HVS) and the Crossbow 6-axis inertial navigation sensor. Each sensor is connected to the ATRV-Jr on-board PC (Pentium II, 350MHz) through a serial port on a Rockeport multiserial port card. On the same PC run the low level control software (the RWI's ReFlex accepting speed commands and returning odometric data) and the CORBA servers, that distribute the sensor data over the network. The high level control software, written in C++ language, is a client program that runs on a notebook (Pentium II at 366MHz) that interacts with the ATRV-Jr using TCP/IP over Ethernet link. The experiment here reported has been conducted in the parking lot of our Department (Fig. 8). The navigation algorithm described in section IV has been implemented using data coming from the localization filter.

The robot, starting its path in S (see Fig. 8), remains still for 15sec to estimate both the initial bias for the inertial navigation system and the offset for the GPS cartesian position. In this figure the odometric path (dashed) is extremely inaccurate and rapidly diverges while the GPS estimate (plus) has a limited error. The output of the filter (circles) does not coincide with the effective path (not reported) but its maximum deviation has been of 0.5m.

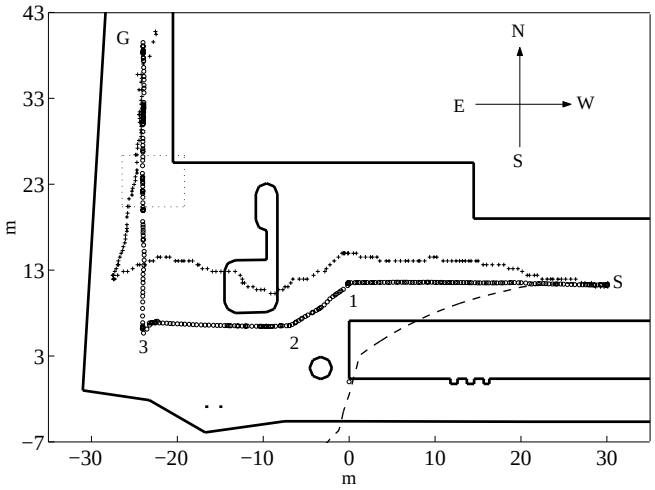

Fig. 8. Robot path in the Department parking lot: the path by the algorithm (circle), GPS (plus) and odometry (dashed line)

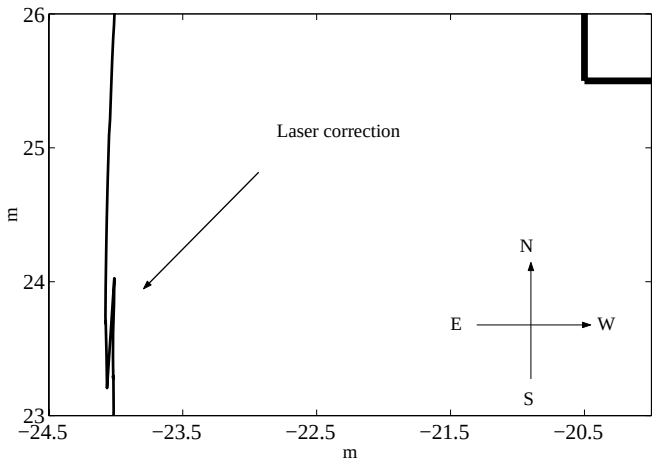

Fig. 9. Laser correction on building corner

After this initialization step, moving with constant speed towards point 1, the robot integrates satellite measures with laser readings but, due to unpredictable obstacles (parked cars) the matching with the map is not always possible. Moreover, in the front direction, walls are too far (more than 8 meters) and the estimated position relies only on GPS with an error that slowly increases. When the robot approaches point 1, and the laser system starts to give a reliable measure that can be matched with the map, the error is reduced from 0.4m to 0.1m. To help the Kalman filter, an additional stop of a few seconds is used to stabilize the estimate configuration. After that, circumnavigating the obstacle, the robot moves to via-points 2 and 3. Although the robot, approaching point 3, has no information from the laser system and uses only GPS data, its position estimate does not appreciably drift towards North: this could be expected due to the big difference with GPS information, but, being the covariance matrix associated to the GPS data greater than $P_{k/k-1}$, the filter output is not greatly influenced. This dominance, with actual gains, would last only for about one minute; after this interval $P_{k/k-1}$ would degrade to the GPS value and the estimate would coincide with it.

In point 3 the West limit of the parking lot is seen by laser system and the longitudinal position is again accurate when the robot starts to move towards the goal G. Along this last segment a singular adjustment occurs: the particularly bad latitude estimate is suddenly fixed as the corner is recognized. In the same figure, the magnification in Fig. 9 shows the discontinuity that has no effect on the control law as stated before.

VI. Conclusion

The elimination of the Selective Availability from the Global Positioning System has made outdoor localization available even using inexpensive receivers. In the present paper an experimental analysis of its performance is reported and it used, together with other sensors, to implement an Extended Kalman Filter for an ATRV Jr robot. The results show that it is very important to have information about the Dilution Of Precision (DOP) or about the satellite geometry to estimate its error. This error also affects the strategy of the planning system: if large errors are expected the trajectory must pass near some easily recognizable environment feature, even if this lengthens the path.

Acknowledgments

This work has been partially supported by *Murst* funds inside RAMSETE project.

References

[1] J. J. Leonard and H. F. Durrant-Whyte, "Mobile robot localization by tracking geometric beacons," *IEEE Trans. on Robotics and Automation*, vol. 7, no. 3, pp. 376–382, 1991.

[2] A. C. Gelb, *Applied Optimal Estimation,* MIT Press, Cambridge, MA, 1994.

[3] J. C. Latombe, *Robot motion planning,* Kluwer Academic Publisher, Boston, MA, 1991.

[4] J. Gonzalez, A. Stenz, and A. Ollero, "An iconic position estimator for a 2D laser rangefinder," *1992 IEEE Int. Conf. on Robotics and Automation*, San Diego, CA, pp. 2646–2651, 1992.

[5] B.Barshan and H.F. Durrant-Whyte, "Inertial navigation system for mobile robots," *IEEE Trans. on Robotics and Automation*, vol. 7,no. 3, pp. 376–382, 1991.

[6] Borenstein, J., Everett, H.R., Feng, L., *'Where am I?' Sensors and Methods for Mobile Robot Positioning* Technical Report, The University of Michigan, 1996. Available from *ftp://ftp.eecs.umich.edu/people/johannb/pos96rep.pdf.*

[7] E. Fabrizi, G. Oriolo, S. Panzieri, G. Ulivi "Enhanced uncertainty modeling for robot localization," *Proc. of 7th Int. Symp. on Robotics with Application (ISORA'98)*, Anchorage, AL, 1998.

[8] E. Fabrizi, G. Oriolo, S. Panzieri, G. Ulivi, "Mobile robot localization via fusion of ultrasonic and inertial sensor," *Proc. of 8th Int. Symp. on Robotics with Application*, Maui, HI, 2000.

[9] E. Fabrizi, S. Panzieri, G. Ulivi, "An integrated sensing-guidance system for a robotized wheelchair," 14th IFAC World Congress, pp. 457-462, Beijing, China, July 5-9, 1999.

[10] B. d'Andréa-Novel, G. Champion, G. Bastin, "Control of nonholonomic wheeled mobile robots by state feedback linearization," Int. J. of Robotic Reasearch, vol. 14, pp. 543–559, 1995.

[11] M. Aicardi, G. Cannata, G. Casalino, G. Indiveri, "On the stabilization of the unicycle model projecting a holonomic solution," *Proc. of 8th Int. Symp. on Robotics with Application,* Maui, HI, 2000.